First-principles calculations of second- and third-order elastic constants for single crystals of arbitrary symmetry

Jijun Zhao, J. M. Winey, and Y. M. Gupta*
Institute for Shock Physics and Department of Physics, Washington State University, Pullman, Washington 99164-2816, USA
(Received 28 September 2006; revised manuscript received 7 December 2006; published 12 March 2007)

The method of homogeneous deformation was combined with first-principles total-energy calculations to provide a general method for determining second- and third-order elastic constants for single crystals of arbitrary symmetry. Lagrangian strain tensors characterized by a single strain parameter are applied to the crystal lattice and the elastic strain energy is calculated from first principles. Second- and third-order elastic constants are obtained from a polynomial fit to the calculated energy-strain relation. Fitting the energy-strain relation, rather than the stress-strain relation, provides a more robust procedure and enables the use of certain first-principles codes where the stress tensor cannot be determined directly. To illustrate the method and to compare with previous work, we calculated the complete set of second- and third-order elastic constants for silicon (cubic lattice). Our results provide better agreement with experimental data than results from previous first-principles calculations. To demonstrate the use of the method for lower-symmetry crystals, second- and third-order elastic constants for α-quartz (trigonal lattice) were calculated and reasonable agreement was obtained with experimental results. Our method is general and can be applied to crystals with low symmetry and/or low yield strength where experimental determination of the third-order elastic constants is difficult.

DOI: 10.1103/PhysRevB.75.094105 PACS number(s): 62.20.Dc, 46.25.−y, 71.15.Nc

I. INTRODUCTION

In the finite-strain theory of elastic deformation, the elastic constants provide a complete description of the elastic response of a solid.[1–3] For single crystals, the second-order elastic constants (SOEC) describe the linear elastic stress-strain response, including the propagation velocity of acoustic disturbances along different crystallographic directions. Higher-order elastic constants, such as third-order elastic constants (TOEC), reflect the nonlinear elasticity of the material, including changes in acoustic velocities due to elastic strain.[2,3] Therefore, both SOEC and TOEC are important parameters for modeling the mechanical response of crystals under high pressure and for simulating large amplitude stress wave propagation in single crystals.[4,5] In addition, SOEC and TOEC values are useful for other purposes, such as the development of ion-electron pseudopotentials[6] or empirical interatomic potentials.[7]

In previous studies, the TOEC for a wide variety of materials have been determined from experiments.[8] However, for crystals with low symmetry and/or low yield stress, such as molecular crystals, obtaining a complete set of TOEC from experimental methods presents significant difficulties. Therefore, it is desirable to be able to determine the TOEC of such materials using theoretical methods. This determination is the focus of the present work.

Several theoretical approaches have been introduced to calculate the TOEC of single crystals. These methods include empirical force-constant models,[9,10] molecular-dynamics simulations using fluctuation formulas,[11,12] and the method of homogeneous deformation based on empirical or first-principles total-energy methods.[1,13] To date, most of the theoretical calculations of TOEC have used the method of homogeneous deformation. In this method, the changes in stress or energy due to a homogeneous strain are calculated. The elastic constants are determined as strain derivatives of the calculated stresses or energy. Previous determinations of TOEC using this method include a variety of calculations for metals using pseudopotentials[14–16] or interatomic potentials.[17,18]

The use of first-principles quantum mechanics calculations to determine TOEC was first introduced by Nielson and Martin.[19,20] Using the stress theorem[21] within density-functional theory, they incorporated first-principles quantum mechanics calculations into the method of homogeneous deformation to obtain the SOEC and TOEC for several crystals having the diamond structure. More recently, the TOEC for several zinc-blende-type crystals have been calculated using first-principles methods.[22]

However, the theoretical developments presented in Ref. 22 were specific to the case of cubic symmetry and there is a need to extend the first-principles calculations to crystals having lower symmetry. Therefore, in this paper, we generalize the previous approach[22] to provide a useful method for calculating the complete set of SOEC and TOEC for single crystals of arbitrary symmetry from first-principles calculations via the application of homogeneous deformations. Our approach, while related to that of Nielsen and Martin,[19,20] contains features that enhance its usefulness for calculations involving complex crystal lattices. We apply our method to cubic silicon and trigonal α-quartz crystals to illustrate its general applicability.

II. THEORETICAL METHOD

In this work, we have combined continuum elasticity theory with first-principles total-energy calculations to calculate the elastic constants of single crystals. Therefore, the basic continuum elasticity theory, the first-principles computational method, and the incorporation of the first-principles calculations into the method of homogeneous deformation used in our work are summarized in the following sections.

A. Continuum elasticity theory

Our method for calculating elastic constants draws upon finite-strain continuum elasticity theory. A detailed discussion regarding the summary presented here can be found in the monographs by Thurston[2] and Wallace.[3]

Let a_i be the initial coordinates of some material element. After a homogeneous elastic deformation, the same material element has coordinates $x_i=x_i(a_j)$. The deformation applied to the material is described by the deformation gradient

$$F_{ij} = \frac{\partial x_i}{\partial a_j}. \tag{1}$$

From the deformation gradients, we define finite Lagrangian strains

$$\eta_{ij} = \frac{1}{2}\sum_k (F_{ki}F_{kj} - \delta_{ij}). \tag{2}$$

Because the Lagrangian strains are symmetric, they contain no information regarding rigid rotation of the material element.

Elastic constants are defined by expanding the internal energy per unit mass U as a Taylor series in elastic strain at constant entropy,[2,3,23]

$$\rho_0 U(\eta_{ij},S) = \rho_0 U(0,S) + \frac{1}{2}\sum_{ijkl} C^S_{ijkl}\eta_{ij}\eta_{kl} + \frac{1}{6}\sum_{ijklmn} C^S_{ijklmn}\eta_{ij}\eta_{kl}\eta_{mn} + \cdots, \tag{3}$$

where ρ_0 is the initial mass density of the material and the initial state is assumed to be stress-free. An expansion in terms of symmetric strains is appropriate because the internal energy is invariant under rigid rotations.[3] The expansion coefficients in the Taylor series of Eq. (3) are the isentropic elastic constants:[2,3,23]

$$C^S_{ijkl} = \rho_0 \left.\frac{\partial^2 U}{\partial\eta_{ij}\partial\eta_{kl}}\right|_{\eta=0} \quad \text{(SOEC)}, \tag{4}$$

$$C^S_{ijklmn} = \rho_0 \left.\frac{\partial^3 U}{\partial\eta_{ij}\partial\eta_{kl}\partial\eta_{mn}}\right|_{\eta=0} \quad \text{(TOEC)}. \tag{5}$$

Similarly, isothermal elastic constants are obtained by expanding the Helmholtz free energy per unit mass at constant temperature,[2,3]

$$\rho_0 F(\eta_{ij},T) = \rho_0 F(0,T) + \frac{1}{2}\sum_{ijkl} C^T_{ijkl}\eta_{ij}\eta_{kl} + \frac{1}{6}\sum_{ijklmn} C^T_{ijklmn}\eta_{ij}\eta_{kl}\eta_{mn} + \cdots. \tag{6}$$

In our first-principles calculations, deformations are applied under isothermal conditions, so that Eq. (6) is applicable. However, our calculations are performed at an effective temperature of 0 K, so that

$$F(\eta_{ij},T=0K) = U(\eta_{ij},T=0K). \tag{7}$$

Because our calculations produce isothermal elastic constants at zero temperature, care must be exercised in comparing with the experimentally determined isentropic elastic constants at room temperature.

To calculate elastic constants using the method of homogeneous deformation, a specified Lagrangian strain tensor η_{ij} is applied to the crystal and the energy for the strained crystal is calculated. The elastic constants are extracted by fitting Eq. (3) [which is equivalent to Eq. (6) at $T=0K$] to the calculated energy-strain results. The first-principles calculation of total energy for the strained crystals is discussed next.

B. First-principles total-energy calculations

In the work presented here, the first-principles calculations were carried out using a plane-wave-pseudopotential method based on density-functional theory (DFT). However, our overall framework places no restriction on the particular first-principles total-energy method being used. Therefore, other first-principles methods, such as Hartree-Fock theory[24] or DFT using atomic basis sets,[24,25] could be used as well. The ability of our approach to accommodate a variety of total-energy methods and basis sets is a feature that is not available in the previous work by Nielson and Martin.[19,20]

All of our DFT plane-wave-pseudopotential calculations were performed using the ABINIT code.[26,27] Within the local-density approximation (LDA), the Ceperley-Alder exchange-correlation[28] parametrized by Perdew and Wang[29] was used. We found that LDA is sufficient to describe the elastic properties of silicon and quartz crystals, since including a gradient correction had no significant effect on the theoretical results. The ion-electron interaction was modeled by Troullier-Martins norm-conserving nonlocal pseudopotentials[30] in the Kleinman-Bylander separable form.[31] The numerical pseudopotential used in this work was generated by the Fhi98PP program.[32] The energy cutoff for the plane-wave basis was 50 Ry for silicon and 160 Ry for quartz. We found that these high energy cutoffs were necessary to provide well-converged values for the elastic constants. The Brillouin zone for silicon and quartz crystals was sampled using $6\times6\times6$ and $4\times4\times4$ grids of **k** points, respectively, following the Monkhorst-Pack scheme.[33] Further increasing either the number of **k** points or the plane-wave energy cutoff did not change our theoretical results.

The equilibrium theoretical crystal structures for silicon and quartz at ambient conditions were determined by minimizing the Hellmann-Feynman force on the atoms and the stress on the unit cell. The modified Broyden algorithm[34,35] was used in the geometry optimization. The tolerance for the total-energy difference in the self-consistent-field calculation was 10^{-9} a.u., and the tolerance for the maximum force in the geometry optimization was 10^{-6} a.u. The known space groups for the silicon and quartz crystals were maintained during the optimization of the initial crystal ground states. However, the homogeneous strains applied in this work typically lowered the symmetry of the crystal. To obtain the unit cell for the strained crystal, the deformation gradient F_{ij} was

applied to the dimensionless crystal lattice vectors $\mathbf{r}_i$ to obtain the deformed lattice vectors $\mathbf{r}_i'$:

$$\mathbf{r}_i' = F_{ij}\mathbf{r}_j. \tag{8}$$

The deformation gradients F_{ij} were determined from the Lagrangian strains η_{ij} by inverting Eq. (2). For a given η_{ij}, the associated deformation gradients F_{ij} are not unique, the various possible solutions differing from one another by a rigid rotation. The lack of a one-to-one relationship between η_{ij} and F_{ij} is not a concern because the calculated energy is invariant under rigid rotations, as discussed in Sec. II A. For a given applied deformation, relaxation of the crystal internal coordinates for the deformed unit cell was performed to obtain the minimized energy for the strained crystal.

C. Calculation of elastic constants

To calculate elastic constants, we introduced Lagrangian strain tensors η_{ij} for cubic and trigonal crystals that result in an energy expansion [Eq. (3)] containing a small number of second- and third-order elastic constants. The η_{ij} used in this work are listed in the Appendix, where we have written the nonzero components of each Lagrangian strain tensor in terms of a single parameter ξ. This feature, though not scientifically profound, has an important practical benefit. Inserting these strains into Eq. (3), the elastic energy per unit mass can be written as an expansion in the strain parameter ξ,

$$\rho_0[U(\xi) - U(0)] = \frac{1}{2}A_2\xi^2 + \frac{1}{6}A_3\xi^3 + O(\xi^4), \tag{9}$$

where $U(0)$ is the energy for the initial state. The coefficients A_2 and A_3 are combinations of second- and third-order elastic constants of the crystal, respectively. These coefficients are obtained by fitting Eq. (9) to plots of energy versus ξ. The use of a single strain parameter ξ enables a one-parameter fit to be performed, even for strain tensors with many nonzero components. For each strain tensor chosen, the calculations were performed by increasing the magnitude of ξ in steps of 0.0025 up to a maximum strain ξ_{max}. Some sample results from this procedure are shown in Fig. 1, which plots the elastic energy density increase $\rho_0[U(\xi)-U(0)]$ for an α-quartz single crystal as a function of ξ for strain tensor (A8) from the Appendix. A polynomial fit using Eq. (9) up to fourth order yields the coefficients $A_2=100.16$ GPa and $A_3=-852.18$ GPa.

The relationship between the coefficients A_2 and A_3 and the second- and third-order elastic constants are presented in Table I for the specific strain tensors listed in the Appendix. Results are shown for both cubic and trigonal crystals. In Table I and in subsequent discussion, we make use of the contracted (Voigt) notation[2,3,23] ($11\rightarrow1$, $22\rightarrow2$, $33\rightarrow3$, $23\rightarrow4$, $13\rightarrow5$, and $12\rightarrow6$) for the tensor indices to write C_{ijkm} and C_{ijklmn} as $C_{\alpha\beta}$ and $C_{\alpha\beta\gamma}$, respectively. For a given single crystal, the number of independent SOEC and TOEC depends on the crystal symmetry,[36] with the number of independent SOEC and TOEC increasing with decreasing crystal symmetry. For example, a cubic crystal has three independent SOEC and six independent TOEC, while a trigonal crystal has six SOEC and 14 TOEC.[36]

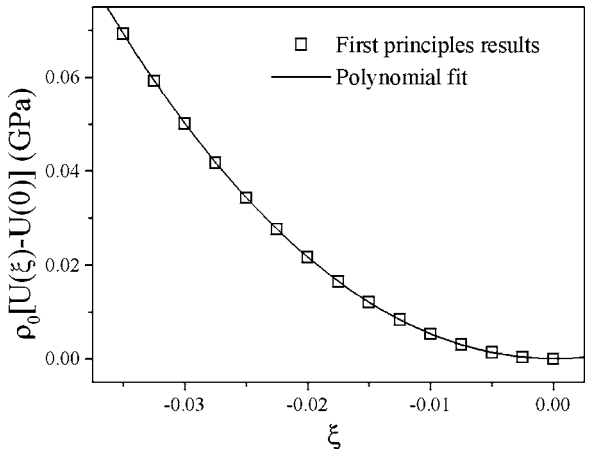

FIG. 1. The calculated change in elastic energy density $\rho_0[U(\xi)-U(0)]$ for α-quartz single crystals as a function of the strain parameter ξ (negative in compression) for strain tensor (A8) defined in the Appendix. A polynomial fit up to fourth order yields $\rho_0[U(\xi)-U(0)]=50.08\xi^2-142.03\xi^3+781.42\xi^4$.

To obtain the complete set of SOEC and TOEC, the fitted values for the coefficients A_2 and A_3 for each strain tensor are equated with the corresponding combination of elastic constants from Table I to generate a system of simultaneous linear equations. The solution of these equations determines the SOEC and TOEC. To obtain a solvable system of equations for the TOEC, the number of applied strain tensors must be as large as the number of independent TOEC of the crystal (six for cubic crystals and 14 for trigonal crystals).

An important parameter in these calculations is the maximum strain parameter ξ_{max} included in the polynomial fit. In our work, the fitted coefficient A_2 for the second-order term was very stable and was almost independent of the range of fitting. However, the coefficient A_3 was more sensitive to ξ_{max}. To illustrate this feature, several TOEC of silicon are plotted in Fig. 2 as a function of the ξ_{max} used in the fitting. The figure shows that the results from the polynomial fit converge for maximum strain parameters ξ_{max} above a certain magnitude (approximately 0.0175 for silicon) and is insensitive to $|\xi_{max}|$ over a certain range (approximately 0.0175–0.030 for silicon). For maximum strain parameters $|\xi_{max}|$ above this range, the contribution from higher-order elastic constants (beyond the TOEC) becomes important so that the fitted coefficients are again sensitive to the ξ_{max} value. Therefore, we chose $|\xi_{max}|=0.025$ for silicon. Similarly, we found $|\xi_{max}|=0.035$ to be a reasonable choice for quartz.

III. APPLICATIONS

A. Silicon

As a specific application of the method, we first performed calculations for the SOEC and TOEC of silicon,

TABLE I. The coefficients A_2 and A_3 in Eq. (9) as combinations of second- and third-order elastic constants for cubic and trigonal crystals. The strain tensors are defined in the Appendix.

Strain	A_2	A_3
	Cubic crystal	
A1	C_{11}	C_{111}
A2	$2C_{11}+2C_{12}$	$2C_{111}+6C_{112}$
A3	$3C_{11}+6C_{12}$	$3C_{111}+18C_{112}+6C_{123}$
A4	$C_{11}+4C_{44}$	$C_{111}+12C_{144}$
A5	$C_{11}+4C_{44}$	$C_{111}+12C_{166}$
A6	$12C_{44}$	$48C_{456}$
	Trigonal crystal	
A1	C_{11}	C_{111}
A2	$2C_{11}+2C_{12}$	$4C_{111}+6C_{112}-2C_{222}$
A3	$2C_{11}+2C_{12}+4C_{13}+C_{33}$	$4C_{111}+6C_{112}+6C_{113}+6C_{123}+6C_{133}-2C_{222}+C_{333}$
A4	$C_{11}+4C_{14}+4C_{44}$	$C_{111}+6C_{114}+6C_{144}+8C_{444}$
A7	C_{11}	C_{222}
A8	C_{33}	C_{333}
A9	$C_{11}+2C_{13}+C_{33}$	$3C_{113}+3C_{133}+C_{222}+C_{333}$
A10	$4C_{44}$	$8C_{444}$
A11	$2C_{11}-2C_{12}+C_{33}$	$6C_{113}-6C_{123}+C_{333}$
A12	$C_{11}-4C_{14}+4C_{44}$	$-6C_{114}-12C_{124}+12C_{155}+C_{222}+8C_{444}$
A13	$C_{11}+4C_{44}$	$12C_{144}+C_{222}$
A14	$C_{33}+4C_{44}$	$C_{333}+12C_{344}$
A15	$C_{11}+2C_{13}+4C_{14}+C_{33}+4C_{44}$	$C_{111}+3C_{113}+6C_{114}+3C_{133}+12C_{134}+12C_{144}+C_{333}+12C_{344}+8C_{444}$
A16	$2C_{11}+2C_{12}+4C_{44}$	$4C_{111}+6C_{112}+12C_{144}+12C_{155}-2C_{222}$

which is a well-studied cubic crystal having the diamond structure. Thus, we could compare our results with previous studies.[19,37,38] After structural optimization, our LDA calculations predict the equilibrium lattice constant to be $a=5.38$ Å, in reasonable agreement with the experimental lattice constant $a=5.43$ Å.[39] In Table II, we compare our calculated elastic constants with experimental results[37,38] and with previous DFT calculations.[19] In the previous calculations, four of the third-order elastic constants (C_{111}, C_{112}, C_{123}, and C_{456}) and one combination ($C_{144}+2C_{166}$) were obtained. Overall, good agreement is found between our theoretical calculations and the experimental results for both SOEC and TOEC. Careful examination shows that our results agree better with the experimental results than the previous DFT calculations.[19] In the case of the SOEC, the pre-

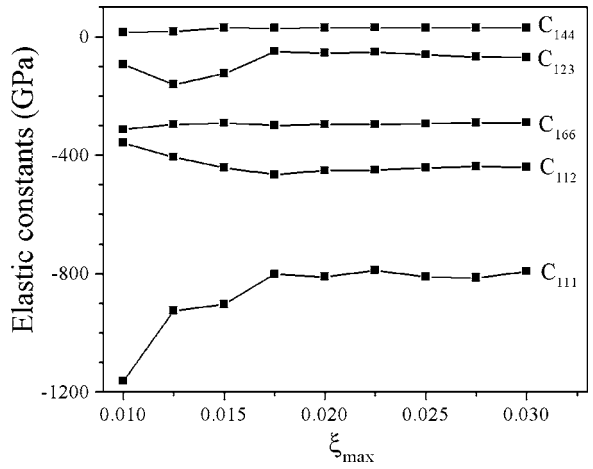

FIG. 2. Third-order elastic constants of silicon as a function of the maximum strain $|\xi_{max}|$ included in the polynomial fit.

TABLE II. Comparison of theoretical and experimental values for the second- and third-order elastic constants for silicon (in units of GPa).

	Present work	LDA[a]	Expt.[b]	Expt.[c]
C_{11}	162.07	159	165.64	165.77
C_{12}	63.51	61	63.94	63.92
C_{44}	77.26	85	79.51	79.62
C_{111}	−810	−750	−795±10	−825±10
C_{112}	−422	−480	−445±10	−451±5
C_{123}	−61	≈0	−75±5	−64±10
C_{144}	31		15±5	12±25
C_{155}	−293		−310±5	−310±10
C_{444}	−61	−80	−86±5	−64±20

[a]Reference 19.
[b]Reference 37.
[c]Reference 38.

vious DFT calculations underestimate C_{11} and C_{12} by about 4% and overestimate C_{44} by about 7%, while the deviation of our theoretical values for C_{11}, C_{12}, and C_{44} from the experimental values[38] is 2.2%, 0.6%, and 2.9%, respectively. For the TOEC, C_{111}, C_{112}, C_{123}, and C_{456} from our calculations are almost within the uncertainty (about ±10 GPa) of the experimental data, while for C_{144} and C_{166}, the discrepancy between the theoretical and experimental values is about 20 GPa. On the other hand, the previous DFT calculations[19] underestimate C_{111} by about 60 GPa and overestimate C_{112} by about 35 GPa. Moreover, the previous calculations predict $C_{123} \simeq 0$, whereas the experimental value is −64 GPa (Ref. 38) or −75 GPa.[37]

B. α-quartz

As an example of the application of our method to noncubic crystals, we performed calculations for α-quartz (SiO_2), because experimental data are available for quartz.[40,41] The crystal structure of α-quartz is trigonal, with space group $P3_121$. The lattice constants for the trigonal unit cell from our calculations are $a=4.85$ Å and $c=5.35$ Å, while the measured lattice constants are $a=4.91$ Å and $c=5.40$ Å.[39] Due to the trigonal symmetry of α-quartz, there are six independent SOEC and 14 independent TOEC.[36] These SOEC and TOEC have been measured in previous experiments.[40,41] However, we are unaware of any previous theoretical calculations for the TOEC of quartz. Using the method described above, 14 strain tensors (see the Appendix and Table I) were applied to the quartz crystal and the complete set of 14 TOEC were determined. Because α-quartz is piezoelectric, elastic constants determined under conditions of constant electric field are distinct from those determined under constant electric displacement. However, in our calculations, as in the experimental work,[41] we assume that the difference between constant field and constant displacement is negligible for the elastic constants of quartz.

The theoretical values for the elastic constants are compared with experimental results in Table III. For the SOEC, our LDA calculations show good agreement with the experimental values (within ~10% for the larger values). For the TOEC, our theoretical calculations reproduce most of the measured elastic constants reasonably well (within ~10% for TOEC with absolute values >200 GPa, or within 30 GPa for many of the smaller TOEC). The discrepancy between theory and experiment for C_{114}, C_{124}, and C_{155} is somewhat larger. The reason for this is not clear because we obtained similar values for these same elastic constants using several different strain tensor combinations. However, the discrepancy might be related to the application of shear strains to the crystal, because the agreement with experimental values is generally better for those elastic constants that result from strain tensors where no shear deformation is involved (i.e., C_{111}, C_{222}, C_{333}, C_{112}, C_{113}, C_{133}, and C_{123}).

Despite the existing discrepancy, the overall reasonable agreement between theoretical and experimental TOEC demonstrates the usefulness of our method for a noncubic crystal. Moreover, our method provides a general approach for determining higher-order elastic constants and is not limited to third-order elastic constants. For example, as shown in Fig. 1, the polynomial coefficient fitted for the fourth-order term yields $C_{3333}=A_4=24(781.42 \text{ GPa})=18\,754$ GPa for quartz, which compares well with an experimental value of $C_{3333}=17\,481$ GPa obtained from shock wave loading experiments.[42] In general, very few higher-order elastic constants (beyond the TOEC) are available experimentally.

TABLE III. Comparison of theoretical and experimental values for the second- and third-order elastic constants for quartz (in units of GPa).

	Present work	Expt.[a]
C_{11}	77.48	86.8
C_{12}	9.65	7.04
C_{13}	9.22	11.91
C_{14}	−18.70	−18.04
C_{33}	100.16	105.75
C_{44}	54.95	58.2
C_{111}	−234	−210±7
C_{222}	−347	−332±8
C_{333}	−852	−815±18
C_{112}	−306	−345±6
C_{113}	13	12±6
C_{114}	−382	−163±5
C_{123}	−264	−294±5
C_{124}	133	−15±4
C_{133}	−325	−312±7
C_{134}	−21	2±4
C_{144}	−150	−134±7
C_{155}	−36	−200±8
C_{444}	−191	−276±17
C_{344}	−80	−110±7

[a]References 40 and 41.

C. Discussion

Overall, the elastic constants obtained from our first-principles calculations agree well with the experimentally measured values. This good agreement is in spite of the fact that our calculations yielded isothermal elastic constants at $T=0$ K, while the experiments measured isentropic elastic constants at room temperature. For silicon, the thermal-expansion coefficient is small relative to metals and ionic solids, which reduces the effect of thermal contributions to the elastic stiffness. For quartz, the thermal-expansion coefficients are larger. However, the difference between the zero temperature, isothermal elastic constants, and the room temperature isentropic elastic constants is likely to remain small because the stiffness change encountered in going from $T=0$ K to room temperature (which typically reduces the elastic constants) tends to offset the changes due to conversion from isothermal to isentropic conditions (which increases the elastic constants).

Regarding the theoretical method, our approach is similar to that used in previous first-principles calculations by Niel-

son and Martin.[19,20] In their calculations, Nielson and Martin determined the TOEC by fitting the calculated crystal stress to a stress-strain relationship obtained by differentiating Eq. (3). As discussed by Nielson,[20] fitting theoretical stresses, rather than the total energy, requires fewer first-principles calculations to determine the SOEC and TOEC. For large systems, this economy of computational effort can be of considerable importance. However, fitting the theoretical stress also has several shortcomings. First, some quantum chemistry or solid-state physics codes [e.g., CRYSTAL,[24] DMOL,[25] and WIEN2K (Ref. 43)] are unable to directly calculate the stress on the crystals, which severely limits their usefulness with the stress-based method. Second, we find that fitting the energy-strain relation is more robust numerically than fitting the stress-strain relation, i.e., the coefficients derived from fitting the calculated total energy are less sensitive to the details of computations compared to the stress-based approach. As we found with quartz crystals, this robustness of the fitting process is of particular importance for lower-symmetry crystals. Furthermore, because of the greater sensitivity of the stress-based procedure, fitting of the elastic constants up to fourth order by this method often produces unreliable results. For example, fitting the stress-strain curve for quartz under the strain tensor (A8) in the Appendix, including terms involving the fourth-order constants, yields $C_{333}=615$ GPa and $C_{3333}=16\,109$ GPa. In contrast, fitting the energy-strain curve yields $C_{333}=852$ GPa and $C_{3333}=18\,754$ GPa, which compare more favorably with the experimental values of $C_{333}=815\pm18$ GPa (Ref. 41) and $C_{3333}=17\,481\pm340$ GPa.[42] Similar behavior is also observed for other TOEC such as C_{111} and C_{222}. Therefore, our energy-based approach, while requiring a larger number of calculations, is more widely applicable than the previous stress-based approach and appears to be more robust for calculations involving lower-symmetry crystals.

IV. SUMMARY AND CONCLUSIONS

A general method has been developed for calculating the second-order elastic constants (SOEC) and third-order elastic constants (TOEC) for single crystals of arbitrary symmetry. In this method, which generalizes previous theoretical work[22] specific to cubic crystals, first-principles total-energy calculations were performed for crystals under various homogeneous elastic deformations, the applied strains being characterized by a single parameter. The elastic constants were extracted from a polynomial fit to the energy versus strain data. Using this method, we determined the SOEC and TOEC for silicon crystals, with our calculations providing superior agreement with experimental data compared to previous first-principles results.[19] To demonstrate the method for a noncubic crystal, the SOEC and TOEC of α-quartz single crystals were determined. With the exception of a few TOEC, the overall agreement with experimental results for quartz is good.

Comparing our approach to previous work, we found that fitting the energy-strain curve results in a more robust procedure compared to fitting the stress-strain curve as was done previously,[19,20] with the energy-strain results being less sensitive to the details of the total-energy calculations. Furthermore, with the energy-strain approach, implementation is possible using first-principles codes that are unable to directly determine the stress in the crystal. The theoretical method presented here is applicable to single crystals of any symmetry. However, it is expected to be particularly useful for crystals with low symmetry and/or low yield strength, where experimental measurement of the complete set of TOEC is difficult.

ACKNOWLEDGMENTS

This work was supported by the Office of Naval Research under Grant No. N00014-01-1-0802 and the Department of Energy under Grant No. DEFG0397SF21388.

APPENDIX

Below, we list the Lagrangian strain tensors η_{ij} used in this work. For silicon crystals, the strain tensors (A1)–(A6) were used, while the strains (A1)–(A4) and (A7)–(A16) were used for α-quartz crystals:

$$\eta_{ij}=\begin{bmatrix}\xi & 0 & 0\\ 0 & 0 & 0\\ 0 & 0 & 0\end{bmatrix}, \tag{A1}$$

$$\eta_{ij}=\begin{bmatrix}\xi & 0 & 0\\ 0 & \xi & 0\\ 0 & 0 & 0\end{bmatrix}, \tag{A2}$$

$$\eta_{ij}=\begin{bmatrix}\xi & 0 & 0\\ 0 & \xi & 0\\ 0 & 0 & \xi\end{bmatrix}, \tag{A3}$$

$$\eta_{ij}=\begin{bmatrix}\xi & 0 & 0\\ 0 & 0 & \xi\\ 0 & \xi & 0\end{bmatrix}, \tag{A4}$$

$$\eta_{ij}=\begin{bmatrix}\xi & \xi & 0\\ \xi & 0 & 0\\ 0 & 0 & 0\end{bmatrix}, \tag{A5}$$

$$\eta_{ij}=\begin{bmatrix}0 & \xi & \xi\\ \xi & 0 & \xi\\ \xi & \xi & 0\end{bmatrix}, \tag{A6}$$

$$\eta_{ij}=\begin{bmatrix}0 & 0 & 0\\ 0 & \xi & 0\\ 0 & 0 & 0\end{bmatrix}, \tag{A7}$$

$$\eta_{ij}=\begin{bmatrix}0 & 0 & 0\\ 0 & 0 & 0\\ 0 & 0 & \xi\end{bmatrix}, \tag{A8}$$

$$\eta_{ij} = \begin{bmatrix} 0 & 0 & 0 \\ 0 & \xi & 0 \\ 0 & 0 & \xi \end{bmatrix}, \quad \text{(A9)}$$

$$\eta_{ij} = \begin{bmatrix} 0 & 0 & 0 \\ 0 & 0 & \xi \\ 0 & \xi & 0 \end{bmatrix}, \quad \text{(A10)}$$

$$\eta_{ij} = \begin{bmatrix} 0 & \xi & 0 \\ \xi & 0 & 0 \\ 0 & 0 & \xi \end{bmatrix}, \quad \text{(A11)}$$

$$\eta_{ij} = \begin{bmatrix} 0 & 0 & 0 \\ 0 & \xi & \xi \\ 0 & \xi & 0 \end{bmatrix}, \quad \text{(A12)}$$

$$\eta_{ij} = \begin{bmatrix} 0 & 0 & \xi \\ 0 & \xi & 0 \\ \xi & 0 & 0 \end{bmatrix}, \quad \text{(A13)}$$

$$\eta_{ij} = \begin{bmatrix} 0 & 0 & \xi \\ 0 & 0 & 0 \\ \xi & 0 & \xi \end{bmatrix}, \quad \text{(A14)}$$

$$\eta_{ij} = \begin{bmatrix} \xi & 0 & 0 \\ 0 & 0 & \xi \\ 0 & \xi & \xi \end{bmatrix}, \quad \text{(A15)}$$

$$\eta_{ij} = \begin{bmatrix} \xi & 0 & \xi \\ 0 & \xi & 0 \\ \xi & 0 & 0 \end{bmatrix}. \quad \text{(A16)}$$

*Electronic address: ymgupta@wsu.edu

[1] M. Born and K. Huang, *Dynamical Theory of Crystal Lattices* (Oxford University Press, London, 1956).
[2] R. N. Thurston, in *Physical Acoustics Principles and Methods*, edited by W. P. Mason and R. N. Thurston (Academic, New York, 1964), Vol. 1A, p. 1.
[3] D. C. Wallace, in *Solid State Physics*, edited by F. Seitz and D. Turnbull (Academic, New York, 1970), Vol. 25, p. 301.
[4] J. M. Winey and Y. M. Gupta, J. Appl. Phys. **96**, 1993 (2004).
[5] J. M. Winey and Y. M. Gupta, J. Appl. Phys. **99**, 023510 (2006).
[6] B. P. Barua and S. K. Sinha, J. Appl. Phys. **49**, 3967 (1978).
[7] S. Chantasiriwan and F. Milstein, Phys. Rev. B **58**, 5996 (1998).
[8] *Second and Higher Order Elastic Constants*, edited by A. G. Every and A. K. McCurdy, Landolt-Börnstein, New Series, Group III, Vol. 29A (Springer, Berlin, 1992).
[9] P. N. Keating, Phys. Rev. **145**, 637 (1966).
[10] P. N. Keating, Phys. Rev. **149**, 674 (1966).
[11] T. Cağin and J. R. Ray, Phys. Rev. B **38**, 7940 (1988).
[12] T. Cağin and B. M. Pettitt, Phys. Rev. B **39**, 12484 (1989).
[13] R. Srinivasan, Phys. Rev. **144**, 620 (1966).
[14] T. Suzuki, A. V. Granato, and J. F. Thomas, Jr., Phys. Rev. **175**, 766 (1968).
[15] J. F. Thomas Jr., Phys. Rev. B **7**, 2385 (1973).
[16] R. Srinivasan and K. S. Girirajan, J. Phys. F: Met. Phys. **3**, 13 (1973).
[17] G. D. Barrera and A. Batana, Phys. Rev. B **47**, 8588 (1993).
[18] G. D. Barrera and A. Batana, Phys. Status Solidi B **179**, 59 (1993).
[19] O. H. Nielsen and R. M. Martin, Phys. Rev. B **32**, 3792 (1985).
[20] O. H. Nielsen, Phys. Rev. B **34**, 5808 (1986).
[21] O. H. Nielsen and R. M. Martin, Phys. Rev. B **32**, 3780 (1985).
[22] J. Sörgel and U. Scherz, Eur. Phys. J. B **5**, 45 (1998).
[23] K. Brugger, Phys. Rev. **133**, A1611 (1964).
[24] C. Pisani, in *Lecture Notes in Chemistry*, edited by C. Pisani (Springer-Verlag, Berlin, 1996), pp. 47–75.
[25] B. Delley, J. Chem. Phys. **92**, 508 (1990).
[26] The ABINIT code is a common project of the Université Catholique de Louvain, Corning Incorporated, and other contributors, http//www.abinit.org
[27] X. Gonze, J.-M. Beuken, R. Caracas, F. Detraux, M. Fuchs, G.-M. Rignanese, L. Sindic, M. Verstraete, G. Zerah, F. Jollet, M. Torrent, A. Roy, M. Mikami, P. Ghosez, J. Y. Raty, and D. C. Allan, Comput. Mater. Sci. **25**, 478 (2002).
[28] D. M. Ceperley and B. J. Alder, Phys. Rev. Lett. **45**, 566 (1980).
[29] J. P. Perdew and Y. Wang, Phys. Rev. B **45**, 13244 (1992).
[30] N. Troullier and J. L. Martins, Phys. Rev. B **43**, 1993 (1991).
[31] L. Kleinman and D. M. Bylander, Phys. Rev. Lett. **48**, 1425 (1982).
[32] M. Fuchs and M. Scheffler, Comput. Phys. Commun. **119**, 67 (1999).
[33] H. J. Monkhorst and J. D. Pack, Phys. Rev. B **13**, 5188 (1976).
[34] C. Broyden, Math. Comput. **19**, 577 (1965).
[35] B. Schlegel, J. Comput. Chem. **3**, 214 (1982).
[36] K. Brugger, J. Appl. Phys. **36**, 759 (1965).
[37] J. J. Hall, Phys. Rev. **161**, 756 (1967).
[38] H. J. McSkimin and P. Andreatch, Jr., J. Appl. Phys. **35**, 3312 (1964).
[39] R. W. G. Wyckoff, *Crystal Structures* (Wiley, New York, 1963), Vol. 1.
[40] H. J. McSkimin, P. Andreatch, and R. N. Thurston, J. Appl. Phys. **36**, 1624 (1965).
[41] R. N. Thurston, H. J. McSkimin, and P. Andreatch, J. Appl. Phys. **37**, 267 (1966).
[42] S. C. Jones and Y. M. Gupta, J. Appl. Phys. **88**, 5671 (2000).
[43] K. Schwartz, J. Solid State Chem. **176**, 319 (2003).